

Towards Online Sign Language Recognition and Translation

Ronglai Zuo¹ Fangyun Wei^{2†} Brian Mak¹

¹The Hong Kong University of Science and Technology ²Microsoft Research Asia

{rzuo,mak}@cse.ust.hk

fawe@microsoft.com

Abstract

The objective of sign language recognition is to bridge the communication gap between the deaf and the hearing. Numerous previous works train their models using the well-established connectionist temporal classification (CTC) loss. During the inference stage, the CTC-based models typically take the entire sign video as input to make predictions. This type of inference scheme is referred to as offline recognition. In contrast, while mature speech recognition systems can efficiently recognize spoken words on the fly, sign language recognition still falls short due to the lack of practical online solutions. In this work, we take the first step towards filling this gap. Our approach comprises three phases: 1) developing a sign language dictionary encompassing all glosses present in a target sign language dataset; 2) training an isolated sign language recognition model on augmented signs using both conventional classification loss and our novel saliency loss; 3) employing a sliding window approach on the input sign sequence and feeding each sign clip to the well-optimized model for online recognition. Furthermore, our online recognition model can be extended to boost the performance of any offline model, and to support online translation by appending a gloss-to-text network onto the recognition model. By integrating our online framework with the previously best-performing offline model, TwoStream-SLR, we achieve new state-of-the-art performance on three benchmarks: Phoenix-2014, Phoenix-2014T, and CSL-Daily. Code and models will be available at <https://github.com/FangyunWei/SLRT>.

1. Introduction

Sign languages, also known as signed languages, are visual languages expressed through hand shapes, body movements, and facial expressions. The field of sign language recognition (SLR) [5, 8, 26, 36, 38, 56, 70, 72] has recently garnered significant interest, particularly for its potential in narrowing the communication divide between the hearing and deaf communities. SLR can be divided into two categories: isolated sign language recognition

(ISLR) [26, 34, 37–39, 75] and continuous sign language recognition (CSLR) [8, 29, 45, 50, 69, 72]. ISLR, a supervised classification task, aims to accurately predict the gloss¹ for each isolated sign. In contrast, as no annotations of sign boundaries are provided, CSLR is a weakly supervised task. In this context, a well-optimized model is able to predict a sequence of glosses from a continuous sign video containing multiple signs. In comparison with ISLR, CSLR is more challenging but more practical. The primary objective of this work is to develop an online CSLR system.

Inspired by the significant progress in speech recognition [2, 15, 17, 44], numerous CSLR works utilize the well-established connectionist temporal classification (CTC) loss [15] for model training. In the inference phase, these models typically process the *entire* sign video as input for making predictions. This approach to inference is referred to as offline recognition, as illustrated in Figure 1a. In contrast to modern speech recognition systems, which efficiently recognize spoken words on the fly, the field of sign language recognition still lags behind, primarily due to the absence of practical solutions for online recognition. Although CTC-based approaches can be adapted for online recognition using a sliding window technique, we empirically find that the discrepancy between training (using entire, untrimmed sign videos) and inference (employing short, trimmed sign clips) results in suboptimal performance.

In this paper, we take the first step towards practical online sign language recognition. Instead of training directly with the CTC loss on a CSLR dataset, we optimize an ISLR model using classification losses on a dictionary comprising all glosses within the target CSLR dataset. During the inference phase, for a given sign video stream, we employ a sliding window with a predefined stride on the input stream, and process each video clip through the well-optimized ISLR model to obtain its respective prediction. As a result, training and inference are consistent, both utilizing short video clips as input. However, using a sliding window with a small stride might result in a sign being scanned multiple times in a video stream, leading to repetitive predictions. To address this issue, we introduce an effective post-processing technique

[†]Corresponding author.

¹A gloss is a label associated with an isolated sign.

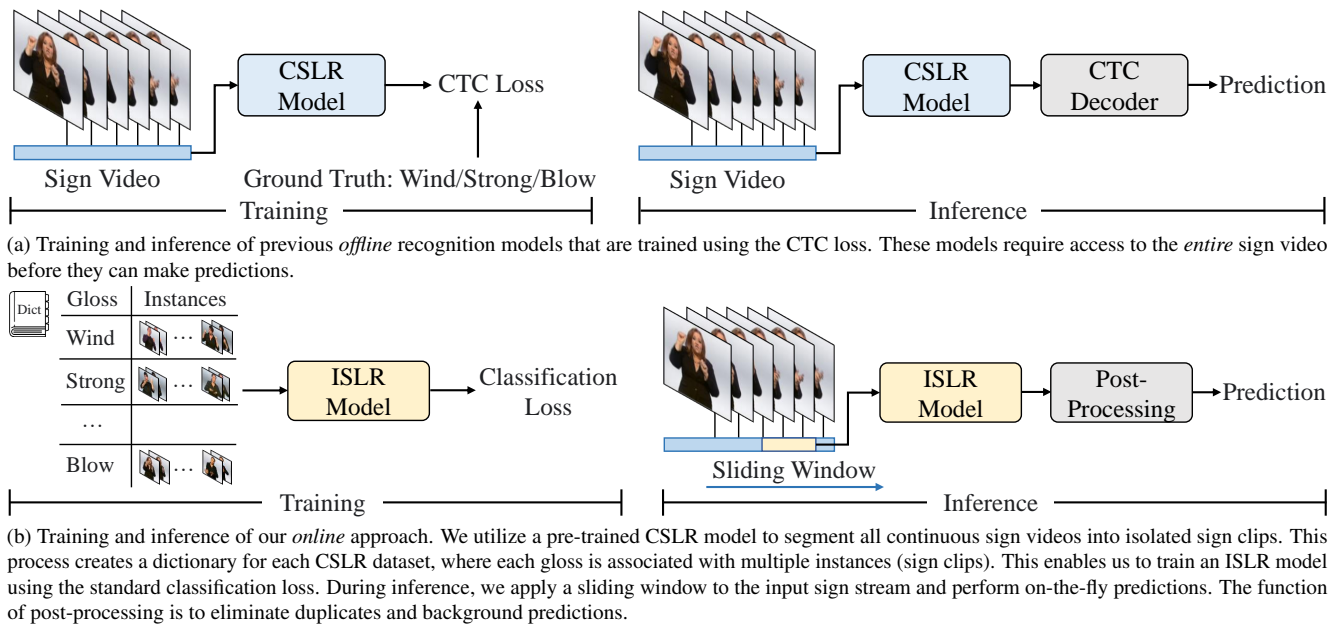


Figure 1. Illustration of (a) the offline recognition scheme and (b) the proposed online framework.

to eliminate duplicate predictions. Additionally, we consider co-articulations, the transitional movements of the body and hands between two consecutive signs in a continuous video. As these movements are typically meaningless, we designate an additional background category for them. Predictions in this category are also discarded during post-processing. Our online method is depicted in Figure 1b.

In our methodology, we train the ISLR model using a sign dictionary. However, extant CSLR datasets such as Phoenix-2014 [36], Phoenix-2014T [5], and CSL-Daily [71] do not include such a dictionary. Fortunately, a pre-trained CSLR model, equipped with the CTC loss, can efficiently segment continuous sign videos into individual isolated signs [11]. Therefore, we employ the leading-edge CSLR model, TwoStream-SLR [8], as the sign segmentor for any CSLR dataset. This approach enables us to create a sign dictionary that aligns with the glossary of the respective CSLR dataset. It is worth noting that the yielded isolated signs² in the dictionary might not represent the exact ground truths. The boundaries of each isolated sign within a continuous stream are inherently ambiguous, posing challenges even for linguistic experts in determining precise sign boundaries. To address this, we augment each isolated sign into a set of augmented signs by trimming the video segments surrounding it. This procedure also substantially enriches the training data.

Different signs typically exhibit various durations. Personal habits of signers, *e.g.*, signing speed, can also amplify this issue. This necessitates the model’s adaptability to variations in sign durations to maintain effectiveness. We introduce a saliency loss, which compels the model to focus

²In this paper, segmented signs are referred to as *isolated signs*.

predominantly on the foreground signs while minimizing the influence of the background co-articulations. The implementation is simple—we adopt an auxiliary classification loss on the pooled feature of the foreground parts.

While our method is primarily developed for online sign language recognition, it also holds potential for facilitating online sign language translation (SLT) and enhancing offline recognition models. Specifically, we implement an additional gloss-to-text network, utilizing the wait- k policy [41, 65] tailored for simultaneous (online) machine translation. This enables online SLT by progressively feeding the gloss predictions produced by our online recognition model into the wait- k gloss-to-text network. Furthermore, drawing from the recent achievements in adapter networks [4, 21, 52, 62], we integrate a lightweight adapter into our frozen online model. We then fuse the features produced by the adapter network with those extracted by a pre-trained offline model (*i.e.*, TwoStream-SLR [8]) to promote the performance of offline recognition models. The resulting model achieves state-of-the-art results on three widely adopted benchmarks: Phoenix-2014 [36], Phoenix-2014T [5], and CSL-Daily [71]. Our contributions can be summarized as follows:

- **One framework.** Instead of training offline SLR models with the CTC loss as the usual practice, we introduce an innovative online SLR framework that slides an ISLR model over a sign video stream. To enhance the ISLR model, we propose several techniques such as sign augmentation and saliency loss.
- **Two extensions.** First, we implement online SLT by integrating a wait- k gloss-to-text network. Second, we extend

the online SLR framework to boost the performance of offline SLR models through the integration of a lightweight adapter.

- **Performance.** By integrating our online framework with the previous best offline model [8], we achieve a new state-of-the-art on three widely used benchmarks: Phoenix-2014 [36], Phoenix-2014T [5], and CSL-Daily [71].

2. Related Works

Sign Language Recognition. Sign language recognition (SLR) is one of the most important research directions in sign language understanding [7, 8, 10, 48, 66, 67, 75]. SLR is categorized into isolated SLR (ISLR), a supervised classification task requiring a model to predict a single gloss from an isolated sign video, and continuous SLR (CSLR), a weakly supervised task where a model is optimized to predict a sequence of glosses from a continuous sign video. Since only sentence-level annotations are provided for CSLR, most CSLR works [7–9, 16, 18, 24, 29, 45, 46, 69, 74] adopt the well-established CTC loss [15], which is proven effective in speech recognition [2, 15, 17, 44], to train their models. These CTC-based models have achieved satisfactory offline recognition performance. For instance, the current best method, TwoStream-SLR [8], achieves a word error rate of 18.8% on the Phoenix-2014 test set. However, there is a notable performance drop in online scenarios due to the discrepancy between training on long, untrimmed videos and inference on short clips. To address this, FCN [9] proposes a fully convolutional network with a small receptive field for preliminary online SLR efforts. However, FCN is still trained on long videos, maintaining the training-inference discrepancy, and its performance remains suboptimal. In our work, we propose a novel approach by training an ISLR model on a sign dictionary, enabling effective online inference through a sliding window strategy.

ISLR is a classification task and has been explored in numerous recent works [22, 26, 31, 34, 37–39, 68, 75]. Some CSLR models [11, 54, 55, 70] adopt the idea of ISLR to iteratively train their feature extractors, a process also known as stage optimization [11]. In this work, our ISLR model not only achieves promising results in online recognition but also boosts the offline models using a lightweight adapter network.

Sign Spotting. The goal of sign spotting is to identify one or multiple desired signs from a continuous sign video. Modern sign spotting works typically rely on extra cues, including external dictionaries [47], mouthings [1], Transformer attention [61], or a combination of them [48]. However, these cues can be either difficult to obtain (*e.g.*, dictionaries) or unreliable (*e.g.*, mouthings). Although sign spotting is closely related to our work, it is typically used to enrich the training source for ISLR and few works validate the spotting task in the context of CSLR.

Online Speech Recognition. Practical online (streaming) speech recognition systems have been the subject of numerous studies [3, 13, 19, 42, 43, 53]. In these studies, model architectures vary, including CNN [53], RNN [13, 19], Transformer [43], and a combination of them [3]. Additionally, multiple optimization frameworks are explored, such as CTC [3, 53], seq2seq [13, 19], or a hybrid of these [42, 43]. Unlike online speech recognition, online sign language recognition remains under-explored. This work takes the first step towards practical online sign language recognition.

3. Method

An overview of our online framework is shown in Figure 2. We first build a sign dictionary with the aid of a sign segmentor, *i.e.*, a pre-trained CSLR model (Section 3.1). Then, we train an ISLR model on this dictionary, employing dedicated loss functions at both the instance and gloss levels (Section 3.2). This is followed by a demonstration of online inference using the optimized ISLR model (Section 3.3). Finally, we present two extensions (Section 3.4): (1) enabling online sign language translation by integrating a wait- k gloss-to-text network; (2) boosting the performance of an offline model using our online model.

3.1. Dictionary Construction

Sign Segmentor. Existing CSLR datasets [5, 36, 71] only provide sentence-level gloss annotations, lacking labels for the temporal boundaries of each isolated sign. Inspired by the observation that a well-trained CTC-based CSLR model can identify the approximate boundaries of the isolated signs in a continuous sign video—by searching the most probable alignment path with respect to the ground truth [11]—we adopt the state-of-the-art CSLR model, TwoStream-SLR [8], as the sign segmentor. This model segments each continuous sign video into a sequence of isolated signs, as depicted in Figure 2a.

Specifically, given a continuous sign video V with T frames and its corresponding gloss label sequence $g = (g_1, \dots, g_N)$ consisting of N glosses, the sign segmentor generates multiple paths associated with the ground truth g . The dynamic time warping (DTW) algorithm [11, 49, 63] can efficiently search for the most probable path $\theta = (\theta_1, \dots, \theta_T)$ in relation to the ground truth g , where $\theta_t \in \{g_i\}_{i=1}^N \cup \{\emptyset\}$ and \emptyset is the blank (background) class. We utilize the background class to model co-articulations between adjacent signs. Upon determining the optimal path θ , which contains frame-wise predictions, we aggregate successive duplicate predictions into an isolated sign. The above process is repeated for each continuous sign video. We collect these segmented signs (pseudo ground truths) to form a dictionary \mathcal{D} . Each sign $s \in \mathcal{D}$ is expressed as a quadruple (V, t_b, t_e, g) , where V is the corresponding continuous sign video, t_b and t_e denote the beginning and ending frame

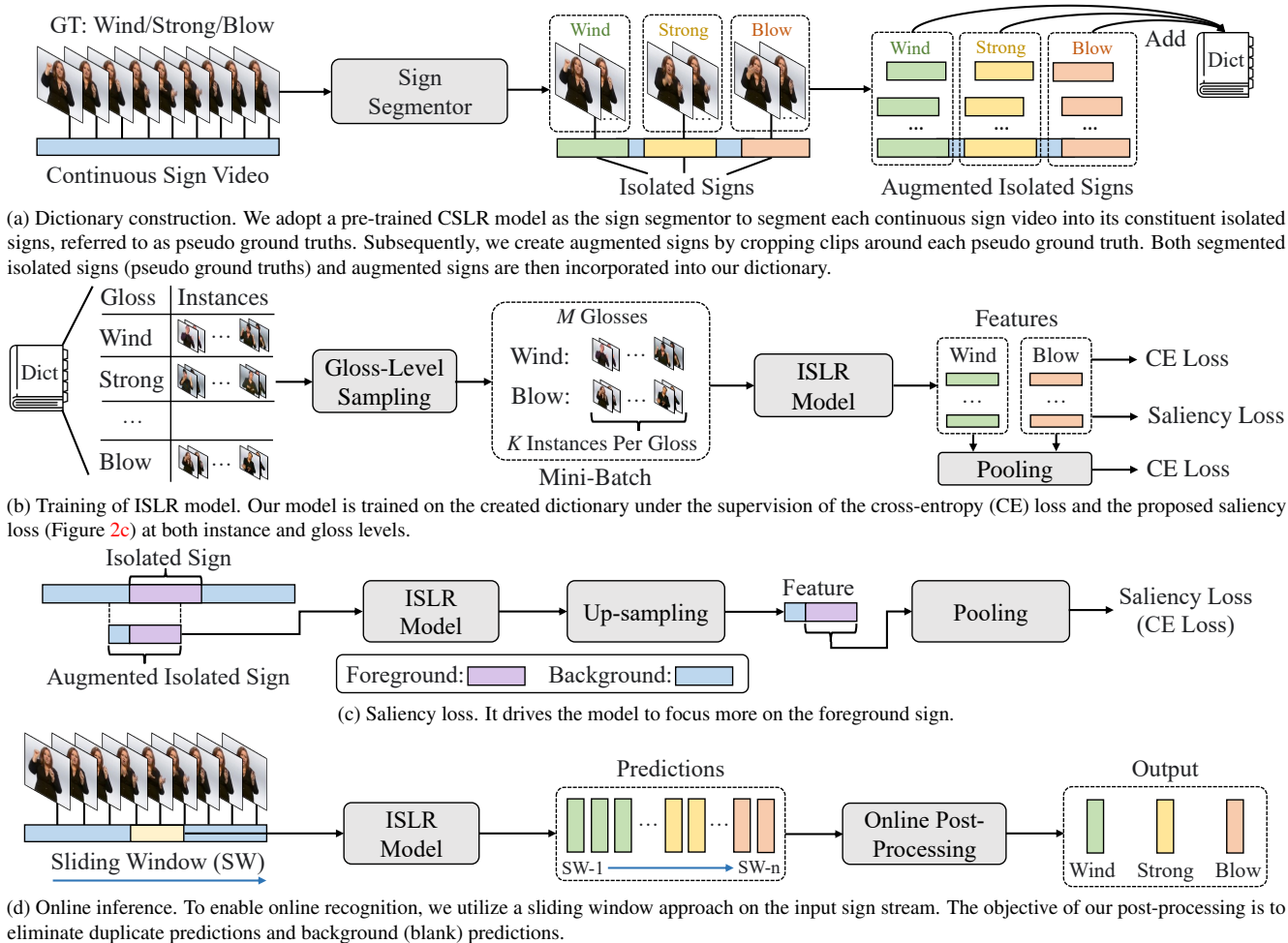


Figure 2. Overview of our methodology.

indexes of sign s in \mathbf{V} , and g is the associated gloss label. Further details can be found in the supplementary materials.

Sign Augmentation. Since the segmented signs are considered pseudo ground truths and their boundaries might not be accurate, we propose a strategy to augment these pseudo ground truth signs. This is done by cropping clips around each $s \in \mathcal{D}$, as shown in Figure 2a. For each pseudo ground truth sign $s = (\mathbf{V}, t_b, t_e, g)$ appearing in a sign video \mathbf{V} , we generate $t_e - t_b + 1$ augmented instances $\{(\mathbf{V}, i - W/2, i + W/2 - 1, g)\}_{i=t_b}^{t_e}$ around s , where W ($W = 16$ by default) is the window size. These yielded instances are then added to the dictionary. As a result, the training source is significantly enriched, and the final sign dictionary is composed of N_g glosses, each of which is associated with a collection of sign instances, including both pseudo ground truth signs $\{s\}$ and augmented signs $\{\hat{s}\}$.

3.2. ISLR Model

This section delineates the training methodology and the associated loss functions utilized for the ISLR model. Following TwoStream-SLR [8], the backbone comprises two

parallel S3D [64] networks, which model RGB sign videos and human keypoints, respectively. The input sign video spans W frames in length. Padding is applied to videos shorter than W frames.

Mini-Batch Formation. In the traditional classification task, instances from a training set are randomly selected to form a mini-batch. This sampling strategy is referred to as instance-level sampling. In this work, we empirically discover that the gloss-level sampling (our default strategy), yields better performance. As illustrated in Figure 2b, we initially sample M glosses from the dictionary. For each gloss, we then sample K instances to form a mini-batch, resulting in an effective batch size of $M \times K$. In our implementation, the K instances sampled for each gloss can be either a pseudo ground truth sign or its augmentations as described in ‘‘Sign Augmentation’’ in Section 3.1. Our technique shares a similar spirit with batch augmentation (BA) [20], which augments a mini-batch multiple times. Our gloss-level sampling differs by employing ‘‘temporally jittered’’ instances around the pseudo ground truth signs to form a training batch, instead of directly augmenting the

pseudo ground truths as in BA. Nevertheless, our sampling strategy still retains the benefits of BA, such as decreased variance reduction.

Loss Functions. Given a mini-batch with a size of $M \times K$, let p_j^i denote the posterior probability of the sample with gloss index $i \in [1, M]$ and instance index $j \in [1, K]$. The classification loss of our ISLR model is composed of two parts: 1) an instance-level cross-entropy loss (\mathcal{L}_{ce}^I) applied across $M \times K$ instances; 2) a gloss-level cross-entropy loss (\mathcal{L}_{ce}^G) applied over M glosses to learn more separable representations. The two losses can be formulated as:

$$\begin{aligned}\mathcal{L}_{ce}^I &= -\frac{1}{M \times K} \sum_{i=1}^M \sum_{j=1}^K \log p_j^i, \\ \mathcal{L}_{ce}^G &= -\frac{1}{M} \sum_{i=1}^M \log \frac{1}{K} \sum_{j=1}^K p_j^i.\end{aligned}\quad (1)$$

Saliency Loss. Our ISLR model processes sign clips with a fixed length, but the foreground regions in these clips can vary. To address this, we devise a saliency loss that encourages the model to prioritize the foreground sign and disregard the background signs (co-articulations). An illustration of the proposed saliency loss is shown in Figure 2c. In detail, for a training sample $\hat{s} = (\mathbf{V}, \hat{t}_b, \hat{t}_e, g)$, which is an augmented instance of pseudo ground truth $s = (\mathbf{V}, t_b, t_e, g)$, we input it into our ISLR model. This process yields its encoded feature $\mathbf{f} \in \mathbb{R}^{T_s/\alpha \times C}$, where $T_s = \hat{t}_e - \hat{t}_b + 1$ is the clip length, $\alpha = 8$ is the down-sampling factor, and C denotes the channel dimension. Next, we up-sample \mathbf{f} to $\mathbf{f}_u \in \mathbb{R}^{\beta T_s/\alpha \times C}$ using an up-sampling factor β ($\beta = 4$ by default). The overall scaling factor thus becomes β/α . Without loss of generality, assuming that $\hat{t}_b \leq t_b \leq \hat{t}_e \leq t_e$, the foreground area starts from the t_b -th frame and ends at the \hat{t}_e -th frame. We then can generate the foreground feature $\mathbf{f}_f \in \mathbb{R}^C$ by pooling $\mathbf{f}_u[[\beta t_b/\alpha] : \lfloor \beta \hat{t}_e/\alpha \rfloor, :]$ along the temporal dimension.

Finally, the saliency loss \mathcal{L}_s is implemented as a cross-entropy loss over the probability yielded from \mathbf{f}_f . Similar to \mathcal{L}_{ce}^I and \mathcal{L}_{ce}^G , our saliency loss is imposed at both instance and gloss levels, denoted as \mathcal{L}_s^I and \mathcal{L}_s^G , respectively.

Overall Loss Function. It is implemented as the summation of the classification loss and the saliency loss at both instance and gloss levels: $\mathcal{L} = \mathcal{L}_{ce}^I + \mathcal{L}_{ce}^G + \mathcal{L}_s^I + \mathcal{L}_s^G$.

3.3. Online Inference

As shown in Figure 2d, the online inference is implemented using a sliding-window (SW) strategy with a stride of S . Generally, sliding-window approaches produce duplicate predictions, as they may scan the same sign multiple times. Therefore, post-processing is always necessary. The pseudo code of our online post-processing is provided in Algorithm 1. The algorithm has two key functions: (1) voting-based deduplication (Line 12), and (2) background elimination

Algorithm 1 Post-processing for online inference

```

1: Input: ISLR model  $\mathcal{M}$ ; sliding window size  $W$ ; sliding
   stride  $S$ ; voting bag size  $B$ 
2: Output: Post-processed predictions
3:  $i \leftarrow 0$ 
4:  $raw \leftarrow \text{Queue}(maxsize = B)$   $\triangleright$  Raw predictions
5:  $temp \leftarrow \emptyset$   $\triangleright$  Variable to store last voting result
6:  $output \leftarrow [\emptyset]$   $\triangleright$  Post-processed predictions
7: while receive new frames do
8:    $V \leftarrow \text{concat}(frame_i, \dots, frame_{i+W-1})$ 
9:    $p \leftarrow \arg \max(\mathcal{M}(V))$ 
10:   $raw.push(p)$ 
11:  if  $raw.full()$  then
12:     $p_v \leftarrow \text{voting}(raw)$   $\triangleright$  Majority voting
13:    if ( $p_v \neq \emptyset$ ) and ( $p_v \neq output[-1]$  or  $temp =$ 
    $\emptyset$ ) then  $\triangleright [-1]$  denotes the last element
14:       $\text{print}(p_v)$   $\triangleright$  Output online predictions
15:       $output.append(p_v)$ 
16:    end if
17:     $temp \leftarrow p_v$ 
18:     $raw.pop()$ 
19:  end if
20:   $i \leftarrow i + S$ 
21: end while
22: return  $output[1:]$   $\triangleright$  Output final predictions

```

(Line 13). We build a simple deduplicator based on majority voting: we collect predictions from B SWs to form a voting bag, and output the predicted class that appears more than $B/2$ times. If no class meets this criterion, the bag yields a background class \emptyset . Finally, we eliminate background predictions and merge non-background predictions; for instance, $\{A, \emptyset, \emptyset\} \rightarrow \{A\}$ and $\{A, A, A\} \rightarrow \{A\}$.

3.4. Extensions

Online Sign Language Translation. As shown in Figure 3, we append an additional gloss-to-text network [8] with the wait- k policy [41] onto our online SLR model to enable online SLT. This wait- k policy enables text predictions after seeing k glosses ($k = 2$ following [65]). During the inference phase, gloss predictions produced by our online SLR model are sequentially input into the well-optimized gloss-to-text network, to produce translation results.

Promote Offline Models with Online Model. Our model, primarily dedicated to online SLR, can also enhance the performance of offline models. As shown in Figure 4, consider two well-optimized SLR models: our online model and an existing offline model. Let \mathbf{f} and \mathbf{g} denote the features extracted by the online model and the offline model, respectively. Typically, the temporal and channel dimensions of \mathbf{f} and \mathbf{g} are different. To align the dimensions of \mathbf{f} with those of \mathbf{g} , we attach a lightweight adapter net-

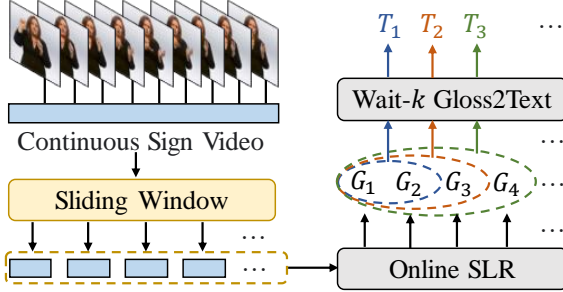


Figure 3. Appending an additional gloss-to-text network with the wait- k policy onto our online SLR model enables online SLT. Circles and arrows distinguished by varied colors indicate translation outcomes at distinct timings.

work—comprising a down-sampling layer and a 2-layer MLP—to the online model. This network projects \mathbf{f} to $\bar{\mathbf{f}}$, matching the dimension of \mathbf{g} . We then integrate $\bar{\mathbf{f}}$ and \mathbf{g} using a weighted sum operation to generate the fused feature $\mathbf{f}_{fuse} = \lambda \cdot \bar{\mathbf{f}} + (1 - \lambda) \cdot \mathbf{g}$, where λ is a trade-off hyper-parameter set to 0.5 by default. Finally, \mathbf{f}_{fuse} is fed into a classification head with the CTC loss as the training objective. The training is extremely efficient since the parameters of both online and offline models are frozen. We adopt TwoStream-SLR [8] as our offline model due to its exceptional performance.

4. Experiments

4.1. Implementation Details

Datasets. We evaluate our method on three widely-adopted CSLR datasets: Phoenix-2014 (P-2014) [36], Phoenix-2014T (P-2014T) [5], and CSL-Daily [71]. *Phoenix-2014* is a German sign language dataset consisting of 5,672/540/629 samples in the training, development (dev), and test set, respectively, with a vocabulary size of 1,081 glosses. *Phoenix-2014T* is an extension of Phoenix-2014, which consists of 1,066 glosses and 7,096/519/642 samples in the training, dev, and test set. *CSL-Daily* is the latest Chinese sign language dataset with a vocabulary size of 2,000 glosses. There are 18,401/1,077/1,176 samples in its training, dev, and test set.

Evaluation Metrics. Following [8, 45, 72], we use word (gloss) error rate (WER), which measures the dissimilarity between the prediction and the ground truth, as the evaluation metric for CSLR. A lower WER indicates better performance. Besides, we also report the performance of our ISLR model on the segmented isolated signs (pseudo ground truths) from the dev and test set as a reference. We report per-instance/class top-1/5 accuracy following [26, 38, 75]. For the translation task, we report BLEU-4 [8].

Training. Following TwoStream-SLR [8], we build our ISLR model using a two-stream architecture that processes both RGB sign videos and their corresponding keypoint heatmaps to interpret sign languages. We use S3D [64] as the backbone. A temporal average pooling layer is appended

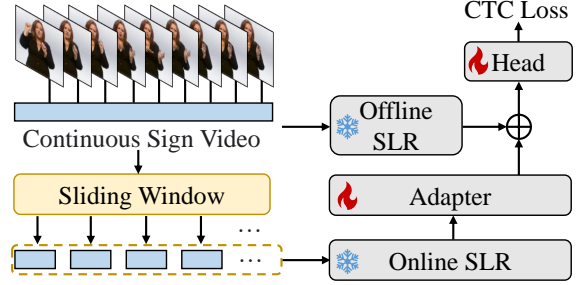


Figure 4. Boosting an offline model with our online model.

onto the network to obtain the clip-level representations. We train our ISLR model with an effective batch size of 4×6 (4 glosses and 6 instances per gloss), for 100 epochs. During sampling, glosses from different videos are treated independently. This strategy is designed to maximize the utilization of the training videos. We use a cosine annealing schedule and an Adam optimizer [35] with a weight decay of $1e^{-3}$ and an initial learning rate of $6e^{-4}$. When fine-tuning the adapter network and classification head, we use a smaller learning rate of $1e^{-4}$ and fewer epochs of 40. We set $\lambda = 0.5$.

Inference. Online inference is implemented using a sliding window approach. We set $W = 16, S = 1, B = 7$ in Algorithm 1. For both offline inference and CTC-based online inference, a CTC decoder with a beam width of 5 is used following [8]. More details and studies on hyper-parameters are available in the supplementary materials.

4.2. Comparison with State-of-the-art Methods

Online Recognition. Almost all previous CSLR works are trained under the supervision of the CTC loss [15]. During inference, these approaches generally process an *entire* sign video (thus, they are considered offline recognition) to generate predictions. These CTC-based approaches can be simply adapted to support online recognition by employing a sliding window strategy to the input sign stream. To decode the predictions of the current window U , the initial step involves feeding U into the CSLR model, which yields a probability map \mathbf{P} . The process of producing the prediction of U is facilitated by the CTC decoder, which considers \mathbf{P} and the last decoding state of the preceding window. Refer to the original implementation [15, 51] for more details. We implement the online inference for the previously best-performing offline model, TwoStream-SLR [8]. The comparison with the online TwoStream-SLR is shown in Table 1. The performance of online TwoStream-SLR significantly degrades compared to its offline counterpart. We hypothesize that this decline in performance is due to the discrepancy between training (on untrimmed sign videos) and inference (on short sign clips). Even using a larger window size of 40, the performance gap remains over 5% on Phoenix-2014 and 18% on CSL-Daily. This gap is particularly pronounced

Method	Window Size	P-2014		P-2014T		CSL-Daily	
		Dev	Test	Dev	Test	Dev	Test
FCN* [9]	40	29.2	28.9	29.0	29.6	44.7	44.7
	32	30.5	30.2	30.4	30.8	48.9	50.2
	24	32.5	32.8	32.9	34.7	55.6	56.3
	16	36.5	36.4	38.8	39.1	72.3	72.8
TwoStream-SLR [8]	40	23.6	23.7	23.1	23.9	43.0	43.7
	32	25.1	25.0	24.7	26.0	52.7	53.7
	24	26.8	26.6	28.8	29.6	68.4	69.2
	16	30.3	31.6	38.4	39.3	101.4	103.3
Ours	16	22.6	22.1	22.2	22.1	30.2	29.3

Table 1. Comparison with other *online* SLR methods across three benchmarks. With the aid of a sliding window, the TwoStream-SLR [8] (state-of-the-art offline model) achieves online recognition capabilities. *: Due to the unavailability of the source code, we reimplement FCN [9], a preliminary attempt for online SLR. We report their performance using the WER% metric.

Method	Window Size	P-2014T		CSL-Daily	
		Dev	Test	Dev	Test
SimulSLT [65]	Dynamic	22.85	23.14	-	-
TwoStream [8]	40	22.80	22.64	18.54	17.98
	32	22.23	22.01	16.32	16.23
	24	22.19	19.92	13.66	13.49
	16	18.36	18.81	10.40	9.98
Ours	16	23.75	23.69	21.20	20.63

Table 2. Comparison with other *online* SLT methods on two benchmarks. For fair comparison, we use the same wait- k gloss-to-text network for both TwoStream Network [8] and our method.

on CSL-Daily, which we attribute to the longer duration of test videos in CSL-Daily. In contrast, our method directly optimizes an ISLR model and feeds each sliding window into this well-optimized model during inference, thereby aligning training and inference processes. Our approach outperforms online TwoStream-SLR with a window size of 16 by 9.5/17.2/74.0% across the three datasets.

FCN [9] presents a preliminary attempt for online SLR, using a fully convolutional network with a small receptive field. However, its evaluation lacks real-world applicability. The authors simulate the online scenario by either concatenating multiple sign videos or splitting a single video into a predefined number of chunks. To ensure a fair comparison under a realistic scenario, we reimplement FCN and achieve offline recognition WERs of 23.9/24.2% and 23.0/24.5% on Phoenix-2014 and Phoenix-2014T, respectively. These results are comparable to those reported in the original FCN paper [9]. When evaluated in the online context, our model consistently outperforms FCN across all three benchmarks, as shown in Table 1.

Online Translation. The pioneering effort in online SLT is made by SimulSLT [65]. Our approach diverges from SimulSLT in three main aspects: 1) Instead of using a masked Transformer like SimulSLT to encode sign videos, we incorporate an ISLR model for encoding sign clips; 2) For

Method	P-2014		P-2014T		CSL-Daily	
	Dev	Test	Dev	Test	Dev	Test
Joint-SLRT [6]	-	-	24.6	24.5	33.1	32.0
FCN [9]	23.7	23.9	23.3	25.1	33.2	33.5
SignBT [71]	-	-	22.7	23.9	33.2	33.2
STMC [70]	21.1	20.7	19.6	21.0	-	-
SMKD [18]	20.8	21.0	20.8	22.4	-	-
C ² SLR [73]	20.5	20.4	20.2	20.4	31.9	31.0
PCMA [25]	20.2	20.0	18.8	20.0	29.4	28.7
SignBERT+ [26]	19.9	20.0	18.8	19.9	-	-
CVT-SLR [69]	19.8	20.1	19.4	20.3	-	-
TLP [27]	19.7	20.8	19.4	21.2	-	-
CoSign [32]	19.7	20.1	19.5	20.1	28.1	27.2
AdaBrowse+ [30]	19.6	20.7	19.5	20.6	31.2	30.7
SEN [28]	19.5	21.0	19.3	20.7	31.1	30.7
CorrNet [29]	18.8	19.4	18.9	20.5	30.6	30.1
TwoStream-SLR [8]	18.4	18.8	17.7	19.3	25.4	25.3
Ours	17.9	18.0	17.2	18.6	24.8	24.4

Table 3. Comparison with other *offline* SLR methods. The results of [6, 9] on CSL-Daily are reproduced by SignBT [71].

inference, where SimulSLT relies on a boundary predictor to generate word boundaries, we adopt a more straightforward sliding window strategy; 3) Unlike SimulSLT, which is tailored exclusively for online SLT, our model is versatile enough to accommodate both online SLR and SLT. As shown in Table 2, by integrating the wait- k gloss-to-text network into our online SLR model, we observe a superior BLEU-4 score in comparison to SimulSLT. Furthermore, our translation model also outperforms the online TwoStream Network [8], despite using the same gloss-to-text network.

Offline Recognition. As described in Section 3.4 and illustrated in Figure 4, our well-trained online model can enhance the performance of any offline model through the use of an adapter network. We instantiate the offline model with the TwoStream-SLR model due to its superior performance. As shown in Table 3, our approach, which involves fine-tuning only the lightweight adapter network and classification head,

Benchmark	Dev				Test			
	Per-instance		Per-class		Per-instance		Per-class	
	Top-1	Top-5	Top-1	Top-5	Top-1	Top-5	Top-1	Top-5
P-2014	69.5	92.9	49.4	74.5	69.9	93.0	46.6	69.7
P-2014T	76.1	96.6	50.6	77.7	75.7	96.3	48.6	71.8
CSL-Daily	72.9	95.9	57.9	88.2	73.5	96.3	57.9	88.2

Table 4. Performance of our ISLR model on the pseudo ground truths of the three benchmarks.

BG Class	Sign Aug.	Gloss-Level Training		Sal. Loss	Dev	Test
		G-L Samp.	G-L Loss			
					62.6	62.9
✓					49.1	48.4
✓	✓				24.4	24.4
✓	✓	✓			22.7	23.4
✓	✓	✓	✓		22.4	22.6
✓	✓	✓	✓	✓	22.2	22.1

Table 5. Ablation studies for the major components. Each row employs the post-processing. BG: background; Aug.: augmentation; Samp.: sampling; Sal.: saliency.

outperforms the previous best results by 0.8/0.7/0.9% on the test set of the three benchmarks.

4.3. Ablation Studies

Unless otherwise specified, all ablation studies are conducted on the Phoenix-2014T benchmark.

ISLR Performance. In Section 3.1, we segment each continuous sign video from a CSLR training set into a set of isolated signs (pseudo ground truths), forming a dictionary. This same method is applied to segment isolated signs for the dev and test sets of each CSLR dataset. Although these segmented signs do not represent ground truths, they provide a basis for a preliminary evaluation of our ISLR model’s effectiveness. As shown in Table 4, our ISLR model can achieve a per-instance top-1/5 accuracy of around 70/90% on the datasets, suggesting that our ISLR model is capable of recognizing the majority of these isolated signs.

Effects of Major Components. In Table 5, we examine the effect of each major component by progressively adding them to our baseline ISLR model. This baseline model is trained only on pseudo ground truths ($\{s\}$) without the background class, using a single objective function \mathcal{L}_{ce}^I , achieving a WER of 62.6% on the dev set. Then, we introduce the background class into the training, resulting in a significant WER reduction of 13.5%. The largest performance gain comes from sign augmentation; specifically, the model trained on both pseudo ground truths and augmented signs ($\{s\} \cup \{\hat{s}\}$) outperforms the model trained only on $\{s\}$, reducing the WER by 24.7%. Next, our gloss-level training strategy, which uses: 1) a gloss-level sampling strategy that randomly selects M glosses, each comprising K instances; 2) an improved objective function $\mathcal{L}_{ce}^I + \mathcal{L}_{ce}^G$, further decreases the WER to 22.4%. At last, by adding the saliency loss to form the final objective function \mathcal{L} , we achieve WERs

Strategy	Threshold	Dev	Test
IoU	0.5	27.4	27.1
IoU	0.3	23.4	23.6
Center	N/A	22.2	22.1

Table 6. Sign augmentation strategies.

λ	1.0	0.7	0.5	0.3	0.0
Dev	20.5	17.3	17.2	17.4	17.7
Test	20.8	18.7	18.6	18.6	19.3

Table 7. Fusion weight λ .

of 22.2% and 22.1% on the dev and test sets, respectively.

Sign Augmentation. As described in Section 3.1, we augment each segmented isolated sign s (pseudo ground truth) by generating a collection of video clips $\{\hat{s}\}$ around it. These clips are centered within the duration of s . We compare our default strategy with an alternative that employs an intersection-over-union (IoU) criterion [58] to generate augmented sign clips. In this IoU-based strategy, clips $\{\hat{s}\}$ are selected if they meet the condition $\text{IoU}(s, \hat{s}) \geq \gamma$, where γ is a predefined threshold. As shown in Table 6, the IoU-based strategy is sensitive to the threshold variation: a large threshold may result in insufficient augmented signs, particularly for short isolated signs. In contrast, our default strategy does not rely on a predefined threshold and considers each isolated sign s equally.

Feature Fusion. In Table 7, we study the fusion weight λ , when combining the features produced by our online model with an adapter network and the offline model (*i.e.*, TwoStream-SLR [8]) to boost offline recognition (see Section 3.4). Setting $\lambda = 0.0$ degenerates the integrated model to the offline TwoStream-SLR model, whereas $\lambda = 1.0$ indicates that only the features encoded by the online model are used. Note that when $\lambda = 1.0$, the fused model is trained using the original ISLR model (whose parameters are frozen), the adapter network, and the classification head, under the supervision of the CTC loss. Thus, the resulting model performs (20.5/20.8% WER on dev/test set) better than its online counterpart (22.2/22.1% WER on dev/test set), as it considers more contexts during training. We empirically set $\lambda = 0.5$.

5. Conclusion

In this work, we develop a practical online sign language recognition framework. First, we construct a sign dictionary including all glosses present in the training set of a target CSLR dataset. To enrich the training data, we collect augmented signs by cropping clips around each isolated sign in our sign dictionary. To enable online recognition, we train an ISLR model on the dictionary, using both standard classification loss and the introduced saliency loss. With the aid of sliding windows, we perform online recognition by feeding each window into the well-optimized ISLR model on the fly to make predictions. A simple yet efficient post-processing algorithm is introduced to eliminate duplicate predictions. Furthermore, two extensions are proposed: one to online translation and the other to boost offline SLR models. When integrated with the previously best offline model, our framework achieves state-of-the-art performance across

three widely-adopted benchmarks: Phoenix-2014, Phoenix-2014T, and CSL-Daily.

References

- [1] Samuel Albanie, Gül Varol, Liliane Momeni, Triantafyllos Afouras, Joon Son Chung, Neil Fox, and Andrew Zisserman. BSL-1K: Scaling up co-articulated sign language recognition using mouthing cues. In *ECCV*, pages 35–53, 2020. [3](#)
- [2] Dario Amodei, Sundaram Ananthanarayanan, Rishita Anubhai, Jingliang Bai, Eric Battenberg, Carl Case, Jared Casper, Bryan Catanzaro, Qiang Cheng, Guoliang Chen, et al. Deep speech 2: End-to-end speech recognition in english and mandarin. In *ICML*, pages 173–182. PMLR, 2016. [1](#), [3](#)
- [3] Keyu An, Huahuan Zheng, Zhijian Ou, Hongyu Xiang, Ke Ding, and Guanglu Wan. CUSIDE: Chunking, Simulating Future Context and Decoding for Streaming ASR. In *Proc. Interspeech 2022*, pages 2103–2107, 2022. [3](#)
- [4] Ankur Bapna and Orhan Firat. Simple, scalable adaptation for neural machine translation. In *EMNLP*, pages 1538–1548, 2019. [2](#)
- [5] Necati Cihan Camgoz, Simon Hadfield, Oscar Koller, Hermann Ney, and Richard Bowden. Neural sign language translation. In *CVPR*, 2018. [1](#), [2](#), [3](#), [6](#)
- [6] Necati Cihan Camgöz, Oscar Koller, Simon Hadfield, and Richard Bowden. Sign language transformers: Joint end-to-end sign language recognition and translation. In *CVPR*, pages 10020–10030, 2020. [7](#)
- [7] Yutong Chen, Fangyun Wei, Xiao Sun, Zhirong Wu, and Stephen Lin. A simple multi-modality transfer learning baseline for sign language translation. In *CVPR*, pages 5120–5130, 2022. [3](#)
- [8] Yutong Chen, Ronglai Zuo, Fangyun Wei, Yu Wu, Shujie Liu, and Brian Mak. Two-stream network for sign language recognition and translation. In *NeurIPS*, 2022. [1](#), [2](#), [3](#), [4](#), [5](#), [6](#), [7](#), [8](#), [11](#), [12](#), [13](#), [15](#), [16](#)
- [9] Ka Leong Cheng, Zhaoyang Yang, Qifeng Chen, and Yu-Wing Tai. Fully convolutional networks for continuous sign language recognition. In *ECCV*, pages 697–714, 2020. [3](#), [7](#)
- [10] Yiting Cheng, Fangyun Wei, Jianmin Bao, Dong Chen, and Wenqiang Zhang. Cico: Domain-aware sign language retrieval via cross-lingual contrastive learning. In *CVPR*, 2023. [3](#)
- [11] Runpeng Cui, Hu Liu, and Changshui Zhang. A deep neural framework for continuous sign language recognition by iterative training. *IEEE TMM*, PP:1–1, 2019. [2](#), [3](#), [12](#)
- [12] Haodong Duan, Yue Zhao, Kai Chen, Dahua Lin, and Bo Dai. Revisiting skeleton-based action recognition. In *CVPR*, pages 2969–2978, 2022. [12](#)
- [13] Ruchao Fan, Pan Zhou, Wei Chen, Jia Jia, and Gang Liu. An online attention-based model for speech recognition. *Proc. Interspeech 2019*, pages 4390–4394, 2019. [3](#)
- [14] Christoph Feichtenhofer, Haoqi Fan, Jitendra Malik, and Kaifeng He. Slowfast networks for video recognition. In *ICCV*, pages 6202–6211, 2019. [12](#)
- [15] Alex Graves, Santiago Fernández, Faustino Gomez, and Jürgen Schmidhuber. Connectionist temporal classification: Labelling unsegmented sequence data with recurrent neural networks. In *ICML*, page 369–376, 2006. [1](#), [3](#), [6](#), [12](#), [13](#)
- [16] Leming Guo, Wanli Xue, Qing Guo, Bo Liu, Kaihua Zhang, Tiantian Yuan, and Shengyong Chen. Distilling cross-temporal contexts for continuous sign language recognition. In *CVPR*, pages 10771–10780, 2023. [3](#)
- [17] Awni Hannun, Carl Case, Jared Casper, Bryan Catanzaro, Greg Diamos, Erich Elsen, Ryan Prenger, Sanjeev Satheesh, Shubho Sengupta, Adam Coates, et al. Deep speech: Scaling up end-to-end speech recognition. *arXiv preprint arXiv:1412.5567*, 2014. [1](#), [3](#)
- [18] Aiming Hao, Yuecong Min, and Xilin Chen. Self-mutual distillation learning for continuous sign language recognition. In *ICCV*, pages 11303–11312, 2021. [3](#), [7](#)
- [19] Yanzhang He, Tara N Sainath, Rohit Prabhavalkar, Ian McGraw, Raziel Alvarez, Ding Zhao, David Rybach, Anjali Kannan, Yonghui Wu, Ruoming Pang, et al. Streaming end-to-end speech recognition for mobile devices. In *ICASSP*, pages 6381–6385, 2019. [3](#)
- [20] Elad Hoffer, Tal Ben-Nun, Itay Hubara, Niv Giladi, Torsten Hoeffler, and Daniel Soudry. Augment your batch: Improving generalization through instance repetition. In *CVPR*, pages 8129–8138, 2020. [4](#)
- [21] Neil Houlsby, Andrei Giurgiu, Stanislaw Jastrzebski, Bruna Morrone, Quentin De Laroussilhe, Andrea Gesmundo, Mona Attariyan, and Sylvain Gelly. Parameter-efficient transfer learning for nlp. In *ICML*, pages 2790–2799. PMLR, 2019. [2](#)
- [22] Hezhen Hu, Wengang Zhou, and Houqiang Li. Hand-model-aware sign language recognition. In *AAAI*, pages 1558–1566, 2021. [3](#)
- [23] Hezhen Hu, Wengang Zhou, Junfu Pu, and Houqiang Li. Global-local enhancement network for nmf-aware sign language recognition. *ACM transactions on multimedia computing, communications, and applications (TOMM)*, 17(3):1–19, 2021. [13](#)
- [24] Hezhen Hu, Junfu Pu, Wengang Zhou, and Houqiang Li. Collaborative multilingual continuous sign language recognition: A unified framework. *IEEE TMM*, 2022. [3](#)
- [25] Hezhen Hu, Junfu Pu, Wengang Zhou, Hang Fang, and Houqiang Li. Prior-aware cross modality augmentation learning for continuous sign language recognition. *IEEE TMM*, 2023. [7](#)
- [26] Hezhen Hu, Weichao Zhao, Wengang Zhou, and Houqiang Li. SignBERT+: Hand-model-aware self-supervised pre-training for sign language understanding. *IEEE TPAMI*, 2023. [1](#), [3](#), [6](#), [7](#)
- [27] Lianyu Hu, Liqing Gao, Zekang Liu, and Wei Feng. Temporal lift pooling for continuous sign language recognition. In *ECCV*, pages 511–527, 2022. [7](#)
- [28] Lianyu Hu, Liqing Gao, Wei Feng, et al. Self-emphasizing network for continuous sign language recognition. In *AAAI*, 2023. [7](#)
- [29] Lianyu Hu, Liqing Gao, Zekang Liu, and Wei Feng. Continuous sign language recognition with correlation network. In *CVPR*, 2023. [1](#), [3](#), [7](#)
- [30] Lianyu Hu, Liqing Gao, Zekang Liu, Chi-Man Pun, and Wei Feng. Adabrowse: Adaptive video browser for efficient continuous sign language recognition. In *MM*, 2023. [7](#)

- [31] Songyao Jiang, Bin Sun, Lichen Wang, Yue Bai, Kunpeng Li, and Yun Fu. Skeleton aware multi-modal sign language recognition. In *CVPRW*, pages 3413–3423, 2021. **3**
- [32] Peiqi Jiao, Yuecong Min, Yanan Li, Xiaotao Wang, Lei Lei, and Xilin Chen. Cosign: Exploring co-occurrence signals in skeleton-based continuous sign language recognition. In *ICCV*, pages 20676–20686, 2023. **7**
- [33] Sheng Jin, Lumin Xu, Jin Xu, Can Wang, Wentao Liu, Chen Qian, Wanli Ouyang, and Ping Luo. Whole-body human pose estimation in the wild. In *ECCV*, pages 196–214, 2020. **12**
- [34] Hamid Reza Vaezi Joze and Oscar Koller. MS-ASL: A large-scale data set and benchmark for understanding American sign language. In *BMVC*, 2019. **1, 3, 13**
- [35] Diederik P. Kingma and Jimmy Ba. Adam: A method for stochastic optimization. In *ICLR*, 2015. **6, 12**
- [36] Oscar Koller, Jens Forster, and Hermann Ney. Continuous sign language recognition: Towards large vocabulary statistical recognition systems handling multiple signers. *CVIU*, 141:108–125, 2015. **1, 2, 3, 6**
- [37] Taeryung Lee, Yeonguk Oh, and Kyoung Mu Lee. Human part-wise 3d motion context learning for sign language recognition. In *ICCV*, pages 20740–20750, 2023. **1, 3**
- [38] Dongxu Li, Cristian Rodriguez, Xin Yu, and Hongdong Li. Word-level deep sign language recognition from video: A new large-scale dataset and methods comparison. In *WACV*, pages 1459–1469, 2020. **1, 6, 13**
- [39] Dongxu Li, Xin Yu, Chenchen Xu, Lars Petersson, and Hongdong Li. Transferring cross-domain knowledge for video sign language recognition. In *CVPR*, pages 6205–6214, 2020. **1, 3**
- [40] Yinhan Liu, Jiatao Gu, Naman Goyal, Xian Li, Sergey Edunov, Marjan Ghazvininejad, Mike Lewis, and Luke Zettlemoyer. Multilingual denoising pre-training for neural machine translation. *TACL*, 8:726–742, 2020. **12**
- [41] Mingbo Ma, Liang Huang, Hao Xiong, Renjie Zheng, Kaibo Liu, Baigong Zheng, Chuanqiang Zhang, Zhongjun He, Hairong Liu, Xing Li, et al. Stacl: Simultaneous translation with implicit anticipation and controllable latency using prefix-to-prefix framework. In *ACL*, pages 3025–3036, 2019. **2, 5, 12**
- [42] Haoran Miao, Gaofeng Cheng, Pengyuan Zhang, Ta Li, and Yonghong Yan. Online hybrid ctc/attention architecture for end-to-end speech recognition. In *Interspeech*, pages 2623–2627, 2019. **3**
- [43] Haoran Miao, Gaofeng Cheng, Changfeng Gao, Pengyuan Zhang, and Yonghong Yan. Transformer-based online ctc/attention end-to-end speech recognition architecture. In *ICASSP*, pages 6084–6088, 2020. **3**
- [44] Yajie Miao, Mohammad Gowayyed, and Florian Metze. Eesen: End-to-end speech recognition using deep rnn models and wfst-based decoding. In *IEEE Workshop on Automatic Speech Recognition and Understanding (ASRU)*, pages 167–174, 2015. **1, 3**
- [45] Yuecong Min, Aiming Hao, Xiujuan Chai, and Xilin Chen. Visual alignment constraint for continuous sign language recognition. In *ICCV*, pages 11542–11551, 2021. **1, 3, 6**
- [46] Yuecong Min, Peiqi Jiao, Yanan Li, Xiaotao Wang, Lei Lei, Xiujuan Chai, and Xilin Chen. Deep radial embedding for visual sequence learning. In *ECCV*, pages 240–256, 2022. **3**
- [47] Liliane Momeni, Gul Varol, Samuel Albanie, Triantafyllos Afouras, and Andrew Zisserman. Watch, read and lookup: learning to spot signs from multiple supervisors. In *ACCV*, 2020. **3**
- [48] Liliane Momeni, Hannah Bull, KR Prajwal, Samuel Albanie, Gül Varol, and Andrew Zisserman. Automatic dense annotation of large-vocabulary sign language videos. In *ECCV*, pages 671–690, 2022. **3**
- [49] Meinard Müller. Dynamic time warping. *Information retrieval for music and motion*, pages 69–84, 2007. **3, 12**
- [50] Zhe Niu and Brian Mak. Stochastic fine-grained labeling of multi-state sign glosses for continuous sign language recognition. In *ECCV*, pages 172–186, 2020. **1**
- [51] Parlance. <https://github.com/parlance/ctcdecode>. In *Github*, 2021. **6**
- [52] Jonas Pfeiffer, Ivan Vulić, Iryna Gurevych, and Sebastian Ruder. Mad-x: An adapter-based framework for multi-task cross-lingual transfer. In *EMNLP*, pages 7654–7673, 2020. **2**
- [53] Vineel Pratap, Qiantong Xu, Jacob Kahn, Gilad Avidov, Tatiana Likhomanenko, Awni Hannun, Vitaliy Liptchinsky, Gabriel Synnaeve, and Ronan Collobert. Scaling up online speech recognition using convnets. *Proc. Interspeech 2020*, pages 3376–3380, 2020. **3**
- [54] Junfu Pu, Wengang Zhou, and Houqiang Li. Iterative alignment network for continuous sign language recognition. In *CVPR*, pages 4165–4174, 2019. **3**
- [55] Junfu Pu, Wengang Zhou, Hezhen Hu, and Houqiang Li. Boosting continuous sign language recognition via cross modality augmentation. In *ACM MM*, pages 1497–1505, 2020. **3**
- [56] Wendy Sandler and Diane Lillo-Martin. *Sign language and linguistic universals*. Cambridge University Press, 2006. **1**
- [57] Yangyang Shi, Yongqiang Wang, Chunyang Wu, Ching-Feng Yeh, Julian Chan, Frank Zhang, Duc Le, and Mike Seltzer. Emformer: Efficient memory transformer based acoustic model for low latency streaming speech recognition. In *ICASSP*, pages 6783–6787, 2021. **13**
- [58] Zheng Shou, Dongang Wang, and Shih-Fu Chang. Temporal action localization in untrimmed videos via multi-stage cnns. In *CVPR*, pages 1049–1058, 2016. **8**
- [59] Grant Strimel, Yi Xie, Brian John King, Martin Radfar, Ariya Rastrow, and Athanasios Mouchtaris. Lookahead when it matters: Adaptive non-causal transformers for streaming neural transducers. In *ICML*, pages 32654–32676, 2023. **13**
- [60] Ke Sun, Bin Xiao, Dong Liu, and Jingdong Wang. Deep high-resolution representation learning for human pose estimation. In *CVPR*, pages 5693–5703, 2019. **12**
- [61] Gul Varol, Liliane Momeni, Samuel Albanie, Triantafyllos Afouras, and Andrew Zisserman. Read and attend: Temporal localisation in sign language videos. In *CVPR*, pages 16857–16866, 2021. **3**
- [62] Ruize Wang, Duyu Tang, Nan Duan, Zhongyu Wei, Xuan-Jing Huang, Jianshu Ji, Guihong Cao, Daxin Jiang, and Ming Zhou. K-adapter: Infusing knowledge into pre-trained models with adapters. In *ACL Findings*, pages 1405–1418, 2021. **2**
- [63] Fangyun Wei and Yutong Chen. Improving continuous sign language recognition with cross-lingual signs. In *ICCV*, pages 23612–23621, 2023. **3**

- [64] Saining Xie, Chen Sun, Jonathan Huang, Zhuowen Tu, and Kevin Murphy. Rethinking spatiotemporal feature learning: Speed-accuracy trade-offs in video classification. In *ECCV*, pages 305–321, 2018. 4, 6, 11, 12
- [65] Aoxiong Yin, Zhou Zhao, Jinglin Liu, Weike Jin, Meng Zhang, Xingshan Zeng, and Xiaofei He. Simulslt: End-to-end simultaneous sign language translation. In *MM*, pages 4118–4127, 2021. 2, 5, 7, 12
- [66] Biao Zhang, Mathias Müller, and Rico Sennrich. SLTUNET: A simple unified model for sign language translation. In *ICLR*, 2023. 3
- [67] Huaiwen Zhang, Zihang Guo, Yang Yang, Xin Liu, and De Hu. C2st: Cross-modal contextualized sequence transduction for continuous sign language recognition. In *ICCV*, pages 21053–21062, 2023. 3
- [68] Weichao Zhao, Hezhen Hu, Wengang Zhou, Jiaxin Shi, and Houqiang Li. BEST: BERT pre-training for sign language recognition with coupling tokenization. In *AAAI*, 2023. 3
- [69] Jiangbin Zheng, Yile Wang, Cheng Tan, Siyuan Li, Ge Wang, Jun Xia, Yidong Chen, and Stan Z Li. CVT-SLR: Contrastive visual-textual transformation for sign language recognition with variational alignment. In *CVPR*, 2023. 1, 3, 7
- [70] Hao Zhou, Wengang Zhou, Yun Zhou, and Houqiang Li. Spatial-temporal multi-cue network for continuous sign language recognition. In *AAAI*, pages 13009–13016, 2020. 1, 3, 7
- [71] Hao Zhou, Wengang Zhou, Weizhen Qi, Junfu Pu, and Houqiang Li. Improving sign language translation with monolingual data by sign back-translation. In *CVPR*, 2021. 2, 3, 6, 7
- [72] Ronglai Zuo and Brian Mak. C2SLR: Consistency-enhanced continuous sign language recognition. In *CVPR*, 2022. 1, 6
- [73] Ronglai Zuo and Brian Mak. Improving continuous sign language recognition with consistency constraints and signer removal. *arXiv preprint arXiv:2212.13023*, 2022. 7
- [74] Ronglai Zuo and Brian Mak. Local context-aware self-attention for continuous sign language recognition. In *Proc. Interspeech*, pages 4810–4814, 2022. 3
- [75] Ronglai Zuo, Fangyun Wei, and Brian Mak. Natural language-assisted sign language recognition. In *CVPR*, 2023. 1, 3, 6, 13

A. More Implementation Details

A.1. Sign Segmentor

We use a pre-trained CSLR model, TwoStream-SLR [8], to segment continuous sign language videos into a set of isolated sign clips, which are then utilized to train our ISLR model. Below we formulate the segmentation process.

Given a continuous sign video \mathbf{V} comprising T frames and its gloss sequence $\mathbf{g} = (g_1, \dots, g_N)$ consisting of N glosses, the probability of an alignment path $\theta = (\theta_1, \dots, \theta_T)$ with respect to the ground truth \mathbf{g} , where $\theta_t \in \{g_i\}_{i=1}^N \cup \{\emptyset\}$ and \emptyset is the blank (background) class,

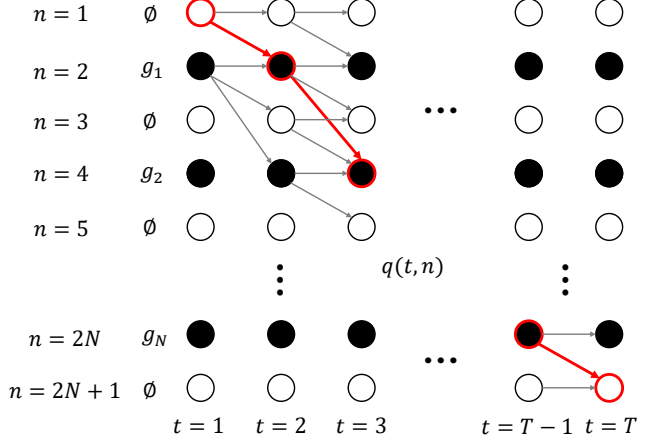


Figure 5. Illustration of the dynamic programming algorithm used to compute $q(t, n)$ (Eq. 4). \emptyset is the blank class, (g_1, \dots, g_N) is the gloss sequence. The red lines denote the optimal path, which is obtained by backtracking from the final gloss that has the maximum probability (Eq. 8). Pseudo code is available in Algorithm 2.

Algorithm 2 Search for the optimal alignment path

- 1: **Input:** Frame-wise probabilities \mathbf{p} ; Extended gloss sequence $\hat{\mathbf{g}}$; Initialized $q(t, 0)$ and $q(1, n)$
 - 2: **Output:** The optimal alignment path $\theta^* = (\theta_1^*, \dots, \theta_T^*)$
 - 3: **for** $n \leftarrow 1$ to $2N + 1$ **do** ▷ Recursive computation
 - 4: **for** $t \leftarrow 2$ to T **do**
 - 5: $q(t, n) = p_t(\hat{g}_n) \max_{f(n) \leq k \leq n} q(t-1, k)$
 - 6: **end for**
 - 7: **end for**
 - 8: $n \leftarrow \arg \max_{k \in \{2N, 2N+1\}} q(T, k)$ ▷ Backtracking
 - 9: $\theta_T^* \leftarrow \hat{g}_n$
 - 10: **for** $t \leftarrow T-1$ to 1 **do**
 - 11: $n \leftarrow \arg \max_{f(n) \leq k \leq n} q(t, k)$
 - 12: $\theta_t^* \leftarrow \hat{g}_n$
 - 13: **end for**
 - 14: **return** $\theta^* = (\theta_1^*, \dots, \theta_T^*)$
-

can be estimated with the conditional independence assumption:

$$p(\theta|\mathbf{V}) = \prod_{i=1}^T p_t(\theta_t), \quad (2)$$

where $p_t(\theta_t)$ denotes the posterior probability that the t -th frame is predicted as the class θ_t . Note that due to the temporal pooling layers in the model’s backbone (S3D [64]), we up-sample the original output probabilities of the CSLR model by a factor of 4 to match the length of the input sign video.

The optimal path is the one with the maximum probability:

$$\theta^* = \arg \max_{\theta \in \mathcal{S}(\mathbf{g})} p(\theta|\mathbf{V}), \quad (3)$$

where $\mathcal{S}(g)$ denotes the set containing all feasible alignment paths with respect to ground truth g . After obtaining the optimal path θ^* , we aggregate successive duplicate predictions into a single isolated sign.

We apply the dynamic time warping (DTW) algorithm [11, 49] to search for the optimal path θ^* . First, we insert blanks to the gloss sequence following the practice in [11, 15]. This process results in an extended gloss sequence of length $2N + 1$: $\hat{g} = (\emptyset, g_1, \emptyset, g_2, \dots, \emptyset, g_N, \emptyset)$. Subsequently, we define $q(t, n)$ as the maximum probability, up to time step t , for the sequence comprising the first n elements of \hat{g} . $q(t, n)$ can be recursively computed as:

$$q(t, n) = p_t(\hat{g}_n) \max_{f(n) \leq k \leq n} q(t-1, k), \quad (4)$$

where

$$f(n) = \begin{cases} n-1 & \text{if } \hat{g}_n = \emptyset \text{ or } \hat{g}_{n-2} = \hat{g}_n \\ n-2 & \text{otherwise} \end{cases} \quad (5)$$

following [15]. The initial conditions of $q(t, n)$ are defined as:

$$q(t, 0) = 0, \quad 1 \leq t \leq T, \quad (6)$$

$$q(1, n) = \begin{cases} p_1(\hat{g}_n) & n = 1, 2 \\ 0 & 2 < n \leq 2N + 1 \end{cases}. \quad (7)$$

The probability of the optimal path can be formulated as:

$$p(\theta^* | \mathbf{V}) = \max_{k \in \{2N, 2N+1\}} q(T, k). \quad (8)$$

Finally, the optimal path θ^* can be obtained by backtracking $p(\theta^* | \mathbf{V})$ in Eq. 8. We provide an illustration and pseudo code of both the recursive computation and backtracking in Figure 5 and Algorithm 2.

A.2. Architecture of the ISLR Model

Following TwoStream-SLR [8], we build our ISLR model using a two-stream architecture, which processes both RGB videos and keypoint heatmaps to more effectively interpret sign languages. The video stream consists of a S3D network [64] for feature extraction, coupled with a head network. The head network includes a temporal average pooling layer and a fully connected layer followed by a softmax layer for computing gloss probabilities. The input video dimensions are $T \times H \times W \times 3$, where T represents the number of frames, and H and W denote the frame height and width, respectively. We standardize H and W to 224 and set T to 16. The S3D network outputs features of size $T/8 \times 1024$ after spatial pooling, which are then input into the head network to generate the gloss probabilities.

Human keypoints are represented as a sequence of heatmaps, following [12], allowing the keypoint stream to

share the same architecture as the video stream. For each sign video, we first use HRNet [60] pre-trained on COCO-WholeBody [33], to generate 11 upper body keypoints, 42 hand keypoints, and 10 mouth keypoints. These extracted keypoints are then converted into heatmaps using a Gaussian function [8, 12]. The input heatmap sequence has dimensions $T \times H' \times W' \times N_k$, where $N_k = 63$ denotes the total number of keypoints, and we set $H' = W' = 112$ to reduce computational cost.

Following TwoStream-SLR [8], we incorporate bidirectional lateral connections [12, 14] and a joint head network to better explore the potential of the two-stream architecture. Lateral connections are applied to the output features of the first four blocks of S3D. Specifically, we utilize strided convolution and transposed convolution layers with a kernel size of 3×3 to align the spatial resolutions of features produced by the two streams. Subsequently, we add the mapped features from one stream to the raw output features of the other stream to achieve information fusion. The joint head network maintains the architecture of the original network in each stream. Its distinctive feature is that it processes the concatenation of the output features of both streams. Refer to the original TwoStream-SLR [8] paper for additional details.

A.3. Training Details

ISLR Model. We train our ISLR model for 100 epochs with an effective batch size of 4×6 , which means that 4 glosses and 6 instances for each gloss are sampled. For data augmentation, we use spatial cropping with a range of [0.7-1.0] and temporal cropping. Both RGB videos and heatmap sequences undergo identical augmentations to maintain spatial and temporal consistency. We employ a cosine annealing schedule and an Adam optimizer [35] with a weight decay of $1e-3$ and an initial learning rate of $6e-4$. Label smoothing is applied with a factor of 0.2. All experiments are run on $8 \times$ Nvidia V100 GPUs.

Wait- k Gloss-to-Text Network. To facilitate online sign language translation, we train an additional gloss-to-text network using the wait- k policy [41], setting $k = 2$ as suggested in [65]. We employ the mBART architecture [40] for this network, owing to its proven effectiveness in gloss-to-text translation [8]. The implementation of the wait- k policy strictly adheres to the guidelines in [41], involving the application of causal masking. The network undergoes training for 80 epochs, starting with an initial learning rate of $1e-5$. To prevent overfitting, we incorporate dropout with a rate of 0.3 and use label smoothing with a factor of 0.2.

Boosting Offline Model. Our online model can boost the performance of offline models with an adapter, as shown in Figure 4 of the main paper. When fine-tuning the adapter network and the classification head, we adopt a smaller learning rate of $1e-4$ and fewer epochs of 40, and the weight

Method	Phoenix-2014		Phoenix-2014T	
	Dev	Test	Dev	Test
NLA-SLR [75]	34.2	33.7	32.9	33.4
Ours	22.6	22.1	22.2	22.1

Table 8. Comparison with the state-of-the-art ISLR method, NLA-SLR [75], in the online SLR context.

Perc. (%)	Dev		Test	
	Dev	Test	Dev	Test
0	45.8	46.8		
20	25.4	25.1		
50	22.5	23.7		
100	22.2	22.1		

(a) Percentage of background samples.

β	Dev	Test
2	22.3	23.2
4	22.2	22.1
8	22.2	22.7

(c) Up-sampling factor (β) in the saliency loss.

B	1	3	5	7	9	11	13
Dev	54.8	27.8	23.0	22.2	23.4	26.1	31.7
Test	57.3	29.0	23.2	22.1	23.2	25.9	31.5

(e) Voting bag size (B).

Table 9. Studies on hyper-parameters.

$\lambda = 0.5$. We adopt the CTC loss [15] as our objective function. Eq. 2 computes the probability of a single alignment path θ . The CTC loss is applied across the set of all feasible alignment paths $\mathcal{S}(g)$ in relation to the ground truth g :

$$\mathcal{L}_{ctc} = -\log \sum_{\theta \in \mathcal{S}(g)} p(\theta|V). \quad (9)$$

B. More Quantitative Results

B.1. Comparison with the SOTA ISLR Method

In this paper, we utilize an ISLR model to fulfill online SLR. Our approach introduces novel techniques for enhancing the training of the ISLR model, including sign augmentation, gloss-level training, and saliency loss. To further verify the effectiveness of our model, we re-implement the leading ISLR method, NLA-SLR [75]. This approach integrates natural language priors into ISLR model training and demonstrates state-of-the-art results across various ISLR benchmarks [23, 34, 38]. However, as shown in Table 8, in the online SLR context, our method significantly outperforms NLA-SLR, evidenced by a notable 11.3% reduction in word

Method	W	WER	AL (ms)	WPL (ms)
TwoStream-SLR [8]	40	23.1	800	94
	32	24.7	640	66
	24	28.8	480	50
	16	38.4	320	31
Ours	16	22.2	320	27

Table 10. Comparison with online TwoStream-SLR in latency on the Phoenix-2014T dev set. W : window size; AL: algorithmic latency; WPL: window processing latency.

error rate (WER) on the Phoenix-2014T test set, affirming the superiority of our ISLR techniques.

B.2. Study on Hyper-Parameters

In Table 9a, we vary the percentage of background samples used from 0% to 100%. We find that using all background samples yields the best performance. This result implies the effectiveness of incorporating the background class in modeling co-articulations.

In a mini-batch, we randomly sample M glosses, with each gloss comprising K instances. The impact of varying M and K is explored in Table 9b.

Our saliency loss aims to enforce the model to focus more on the foreground part. As detailed in Section 3.2 of the main paper, we upsample the feature by a factor of β . We examine various values of β in Table 9c.

We also investigate the optimal size of the sliding window in our proposed online SLR method. Table 9d indicates that a window size of 16 frames is most effective, aligning closely with the average sign duration.

For our online post-processing, we implement majority voting to eliminate duplicates. The influence of the voting bag size B is analyzed in Table 9e. Here, $B = 1$ implies the absence of post-processing. A moderate bag size is preferred as a larger bag might mistakenly drop correct predictions, leading to lower recall. Conversely, a smaller bag might not completely remove duplicates, resulting in lower precision.

B.3. Latency Analysis

Drawing inspiration from previous works in online speech recognition [57, 59], this study presents two types of latencies: algorithmic latency (AL) and window processing latency (WPL). Algorithmic latency is defined as the minimum theoretical delay required to generate a prediction, which relates to the size of the window. Window processing latency, on the other hand, refers to the actual time taken to produce a prediction for a given window input. We compare our approach with the online TwoStream-SLR in Table 10. These evaluations are performed using a single Nvidia V100 GPU. The results demonstrate that our online model exhibits the lowest WER and algorithmic latency. In contrast, the

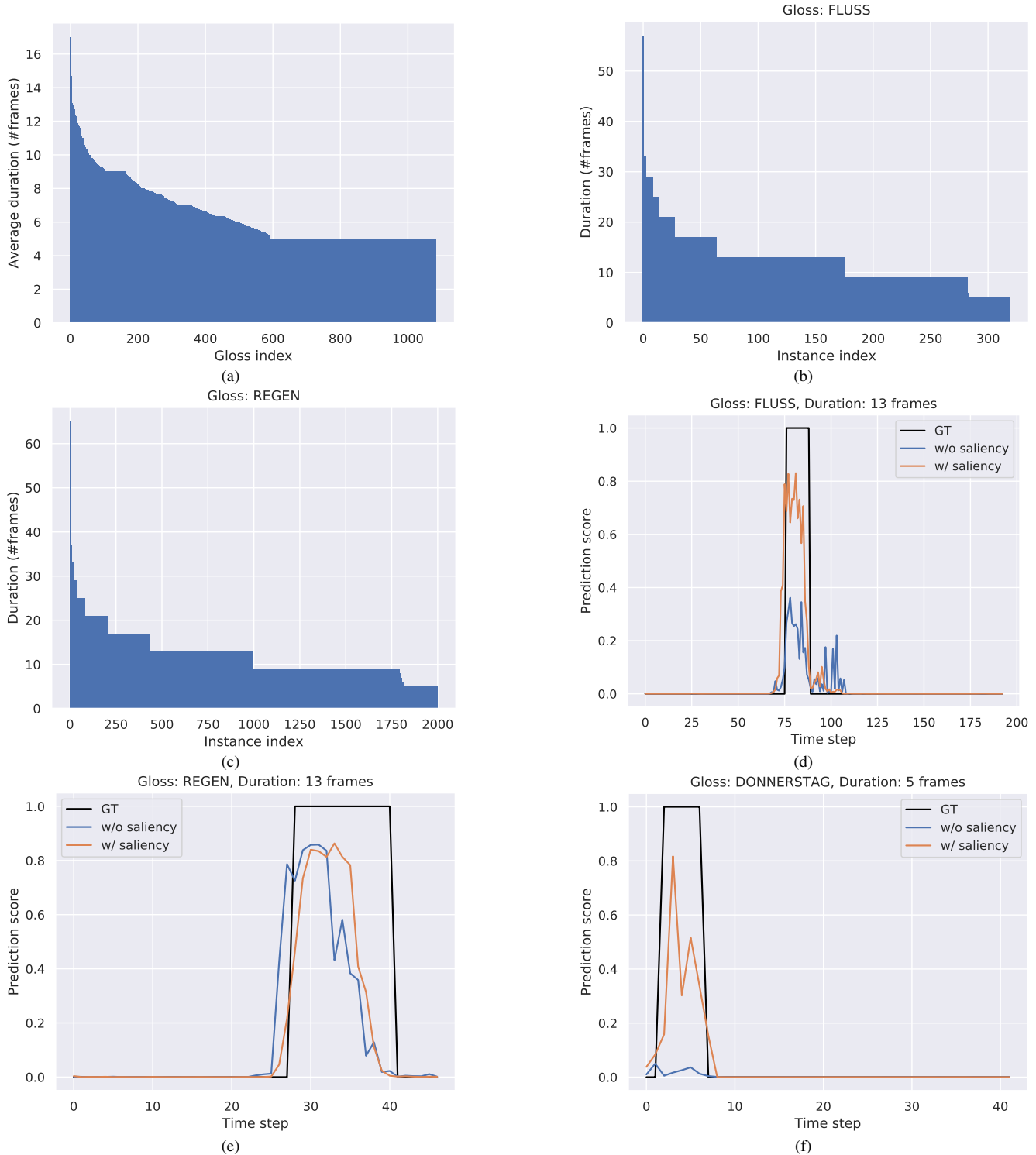


Figure 6. Visualization of sign duration and prediction scores (output probabilities) on the Phoenix-2014T dev set. (a) Statistics of the average duration of each gloss in the vocabulary. To calculate the average duration of a specific gloss, we average the duration of all instances belonging to this gloss. (b)(c) Statistics of the sign duration at the instance level for two randomly selected glosses, namely “FLUSS” and “REGEN”. (d)(e)(f) Window-wise prediction scores of three instances, each belonging to the glosses of “FLUSS”, “REGEN” and “DONNERSTAG”, respectively. Each time step is associated with a window center. We visualize the pseudo ground truths and the predictions made by the models with and without the use of saliency loss.

Example (a)		WER%
Ground truth	TAG SUED MITTE WOLKE KRAEFTIG NEBEL (Day South Mid Cloud Heavy Fog)	-
Prediction ($W = 40$) (TwoStream-SLR [8])	TAG SUED MITTE ***** MEISTENS NEBEL (Day South Mid ***** Mostly Fog)	33.3
Prediction ($W = 16$) (TwoStream-SLR [8])	TAG SUED NEBEL MITTE NEBEL PUEBERWIEGEND NEBEL (Day South Fog Mid Fog Overwhelmingly Fog)	50.0
Prediction ($W = 16$) (Ours)	TAG SUED MITTE WOLKE KRAEFTIG NEBEL (Day South Mid Cloud Heavy Fog)	0.0
Example (b)		WER%
Ground truth	JETZT WETTER WIE-AUSSEHEN MORGEN DIENSTAG NEUNTE FEBRUAR (Now Weather Look Tomorrow Tuesday Ninth February)	-
Prediction ($W = 40$) (TwoStream-SLR [8])	JETZT WETTER WIE-AUSSEHEN MORGEN DIENSTAG WENN NEUNTE FEBRUAR (Now Weather Look Tomorrow Tuesday If Ninth February)	14.3
Prediction ($W = 16$) (TwoStream-SLR [8])	JETZT WETTER JETZT WIE-AUSSEHEN MORGEN DIENSTAG ***** FREUNDLICH (Now Weather Now Look Tomorrow Tuesday ***** Friendly)	42.9
Prediction ($W = 16$) (Ours)	JETZT WETTER WIE-AUSSEHEN MORGEN DIENSTAG NEUNTE FEBRUAR (Now Weather Look Tomorrow Tuesday Ninth February)	0.0
Example (c)		WER%
Ground truth	OST SUEDOST UEBERWIEGEND WOLKE BISSCHEN SCHNEE (East Southeast Mainly Cloud Bit Snow)	-
Prediction ($W = 40$) (TwoStream-SLR [8])	OST ***** MEISTENS WOLKE BISSCHEN SCHNEE (East ***** Mostly Cloud Bit Snow)	33.3
Prediction ($W = 16$) (TwoStream-SLR [8])	REGION KOMMEN OST SUEDOST MEISTENS WOLKE BISSCHEN SCHNEE (Region Come East Southeast Mostly Cloud Bit Snow)	50.0
Prediction ($W = 16$) (Ours)	OST SUEDOST MEISTENS WOLKE BISSCHEN SCHNEE (East Southeast Mostly Cloud Bit Snow)	16.7
Example (d)		WER%
Ground truth	想要健康吸烟不 (Want Be Healthy Smoke No)	-
Prediction ($W = 40$) (TwoStream-SLR [8])	想要身体健康强吸烟不 (Want Be Body Healthy Strong Smoke No)	40.0
Prediction ($W = 16$) (TwoStream-SLR [8])	想我身体健康强吸烟你不 (Want Me Body Healthy Strong Smoke You No)	80.0
Prediction ($W = 16$) (Ours)	想要身体健康吸烟不 (Want Be Body Healthy Smoke No)	20.0
Example (e)		WER%
Ground truth	今天阴大概会下雨 (Today Cloudy Probably Will Rain)	-
Prediction ($W = 40$) (TwoStream-SLR [8])	今天来阴大概会下雨 (Today Come Cloudy Probably Will Rain)	20.0
Prediction ($W = 16$) (TwoStream-SLR [8])	今天来阴你大概会下雨 (Today Come Cloudy You Probably Will Rain)	40.0
Prediction ($W = 16$) (Ours)	今天阴大概会下雨 (Today Cloudy Probably Will Rain)	0.0
Example (f)		WER%
Ground truth	明天考试要带笔不带手机 (Tomorrow Exam Need Bring Pen No Bring Cellphone)	-
Prediction ($W = 40$) (TwoStream-SLR [8])	明天买考试要带你作业不带手机 (Tomorrow Buy Exam Need Bring You Homework No Bring Cellphone)	37.5
Prediction ($W = 16$) (TwoStream-SLR [8])	明天买考试我要带什么快作业不带手机 (Tomorrow Buy Exam Me Need Bring What Quickly Homework No Bring Cellphone)	62.5
Prediction ($W = 16$) (Ours)	明天考试要带作业不带手机 (Tomorrow Exam Need Bring Homework No Bring Cellphone)	12.5

Table 11. Qualitative comparison between the online TwoStream-SLR and our approach on the dev sets of Phoenix-2014T (Example (a,b,c)) and CSL-Daily (Example (d,e,f)), respectively, under the online scenario. We use different colors to represent substitutions, deletions, and insertions, respectively. W denotes the sliding window size.

TwoStream-SLR model’s performance notably diminishes with the adoption of an identical window size of 16 frames.

C. Qualitative Results

C.1. Saliency Loss

In general, a continuous sign video comprises multiple isolated signs linked together with meaningless transitional movements (co-articulations), each serving as a bridge between two adjacent signs. During inference, a given sliding window might include only a portion of an isolated sign, along with segments of one or two co-articulations. The variation in sign duration may also complicate this issue (Figure 6(a)(b)(c)). To enhance the model’s ability to focus on the foreground signs, we introduce the saliency loss. Its objectives are to: 1) drive the model to assign higher activation to each foreground part; 2) encourage the model to learn more discriminative features of the foreground parts. In addition to demonstrating the improvement achieved by integrating the saliency loss, as shown in Table 5 of the main paper, we provide visualization results in Figure 6(d)(e)(f). It is evident that, with the aid of the saliency loss, our model identifies foreground signs more precisely and yields higher activations when the sliding window encounters these signs.

C.2. Comparison of Predictions

As shown in Table 11, we conduct qualitative comparison between the online TwoStream-SLR and our approach, presenting three examples from the dev sets of Phoenix-2014T and CSL-Daily, respectively. It is clear that our proposed online model yields more accurate predictions than the online TwoStream-SLR, even when the latter uses a large window size of 40 frames.

D. Broader Impacts and Limitations

Broader Impacts. Sign languages serve as the primary means of communication within the deaf community. Research on continuous sign language recognition (CSLR) aims to bridge the communication gap between deaf and hearing individuals. While most existing CSLR research has concentrated on enhancing offline recognition performance, the development of an online framework remains largely unexplored. In this paper, we introduce a practical online solution that involves sequentially processing short video clips extracted from a sign stream. This is achieved by feeding these clips into a well optimized model for isolated sign language recognition, thereby enabling online recognition. Our work, therefore, lays the groundwork for future advancements in online and real-time sign language recognition systems.

Limitations. Although we present an effective system for online sign language recognition, our approach has several limitations. First, we use a sign segmentor, *i.e.*, a pre-trained

continuous sign language recognition (CSLR) model, to segment continuous sign videos into several isolated sign clips as pseudo ground truths when building a dictionary. However, the segmented signs may have inaccurate boundaries, introducing unavoidable noise into the subsequent isolated sign language recognition (ISLR) model training. Constructing a dictionary with high-quality samples would benefit our system. Second, our ISLR model adopts the architecture from [8], which jointly models videos and keypoints. Although this achieves superior performance in sign language recognition, the two-stream architecture is inherently heavy. Lightweight sign encoders should be explored more for practical applications. Third, as discussed in TwoStream-SLR [8], imprecise 2D keypoint estimation caused by motion blur, low-quality video, etc., can degrade model performance. A keypoint estimator specifically designed for sign language recognition might mitigate this issue.